

## Tapered fiber Mach–Zehnder interferometer for simultaneous measurement of refractive index and temperature

Ping Lu, Liqiu Men, Kevin Sooley, and Qiying Chen<sup>a)</sup>

*Department of Physics and Physical Oceanography, Memorial University of Newfoundland, St. John's, Newfoundland A1B 3X7, Canada*

(Received 8 February 2009; accepted 17 March 2009; published online 3 April 2009)

An approach to achieve simultaneous measurement of refractive index and temperature is proposed by using a Mach–Zehnder interferometer realized on tapered single-mode optical fiber. The attenuation peak wavelength of the interference with specific order in the transmission spectrum shifts with changes in the environmental refractive index and temperature. By utilizing *S*-band and *C/L*-band light sources, simultaneous discrimination of refractive index and temperature with the tapered fiber Mach–Zehnder interferometer is demonstrated with the corresponding sensitivities of  $-23.188$  nm/RIU (refractive index unit) and  $0.071$  nm/°C, and  $-26.087$  nm/RIU (blueshift) and  $0.077$  nm/°C (redshift) for the interference orders of 169 and 144, respectively. © 2009 American Institute of Physics. [DOI: 10.1063/1.3115029]

*In situ* monitoring of physical, chemical, and biological parameters is of great importance for process control in manufacturing industries, protection of ecosystems, and prevention of global warming. Refractive index (RI) and temperature are the most important parameters in these applications, especially in chemical or food industries for quality control and in biosensing for monitoring molecular bindings or biochemical reactions. Traditionally, the standard technique to measure refractive index is a refractometer, for which many well-known apparatus such as Pulfrich and Abbe refractometers have been used for many decades.<sup>1</sup> Surface plasmon resonance (SPR) has also been adopted for refractive index measurement through evanescent waves in waveguide configurations.<sup>2</sup> However, all these apparatuses are essentially bulky prism systems.

In recent years, fiber-optic sensors have received significant attention for their unique advantages such as immunity to electromagnetic interference, compact size, potential low cost, and the possibility of distributed measurement over a long distance.<sup>3</sup> Earlier work on fiber-optic sensors for refractive index measurement reported metal-coated side-polished fibers, tapered fibers, or multimode fibers with relatively thin cladding layers to excite SPRs.<sup>2,4</sup> Besides the approach with evanescent waves from nanometer fiber tips coated with gold particles,<sup>5</sup> a majority of fiber sensors for refractive index measurement utilized fiber gratings, i.e., long-period gratings (LPGs) and fiber Bragg gratings (FBGs). Recent work that reported refractive index measurement with LPGs are either gold coated,<sup>6</sup> arc-induced phase shifted,<sup>7</sup> asymmetric,<sup>8</sup> or inscribed in air- and water-filled photonic crystal fibers.<sup>9</sup> Reported refractive index measurement with FBGs includes a metal-coated grating in a special single-mode fiber of larger core ( $26\ \mu\text{m}$ ) and thinner cladding ( $30\ \mu\text{m}$ ),<sup>10</sup> a tilted FBG with gold coating in single-mode fiber,<sup>11</sup> and cladding mode resonances of etched-eroded FBG.<sup>12</sup> A few papers reported simultaneous sensing of refractive index and temperature using LPGs, modified FBGs, and hybrid LPG-FBG structures,<sup>13–15</sup> with complicated design, instable system, or

high cost, which restricts their practical applications. The preparation of FBG usually involves photolithographically fabricated phase mask, UV laser, and optical setup for grating inscription. Though LPGs have been revealed to possess a high sensitivity to the refractive index of the ambient medium, the typical full width at half maximum of the resonance peak of a LPG is about tens of nanometers, which limits the measurement accuracy and its multiplexing capability. Most recently, optical refractive index sensors or refractometers based on all-fiber interferometers<sup>16,17</sup> or resonators<sup>18</sup> have received considerable attention for their high sensitivity, absolute detection with wavelength codified information, broad measurement range, and compact size. These fiber interferometric techniques are cumbersome systems with high cost and simultaneous sensing of refractive index and temperature is missing. It is well known that the refractive index of solution has a strong dependence on temperature, and therefore temperature effect should not be neglected in order to obtain an accurate value of the refractive index. In this paper, an in-line one-fiber approach to realize simultaneous measurement of refractive index and temperature is proposed and experimentally demonstrated. Compared with the techniques reported on the interferometers with tapered fibers for sensing applications,<sup>17,19,20</sup> a tapered fiber Mach–Zehnder interferometer (FMZI) has been fabricated on single-mode fiber by using simple fusion splicing in this study. Analysis on the simultaneous measurement of refractive index and temperature has been carried out to verify the experimental results.

A schematic illustration of the experimental setup for simultaneous measurement of refractive index and temperature is shown in Fig. 1(a). Lights from one *S*-band broadband source (BBS) (ASE-FL7200, Thorlabs Inc.) and one dual-band (*C* and *L* band) BBS (EBS-7210, MPB Communications, Inc.) were launched through two tandem fiber tapers and measured by an optical spectrum analyzer (Ando 6315E). Electrical arc method has been adopted in this study to fabricate abrupt tapers in a fiber, and the technique used here is much more simple and convenient which does not rely on specific capabilities of any particular fiber fusion splicer as reported previously.<sup>20</sup> Figure 1(b) shows an abrupt

<sup>a)</sup>Author to whom correspondence should be addressed. Electronic mail: qiyinc@mun.ca.

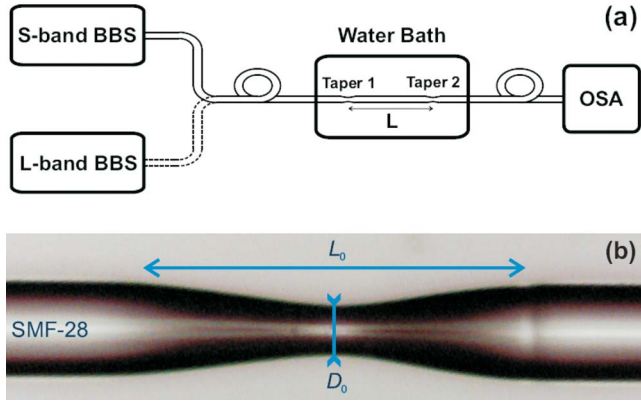


FIG. 1. (Color online) (a) Schematic illustration of the experimental setup. (b) Photograph of a tapered fiber fabricated in this study with parameters of  $D_0=65 \mu\text{m}$  and  $L_0=525 \mu\text{m}$ .

taper fabricated by tapering a standard telecommunication single-mode optical fiber (SMF-28, Corning Inc.) using a FITELE S182A fusion splicer. Two ends of the fiber placed on the prealigned holding plates were stretched and the middle region was heated by arc from the two electrodes inside the fusion splicer. With appropriate arc power, arc duration, and stretching distance, the diameter of the fiber was sharpened to a waist diameter  $D_0$  of  $65 \mu\text{m}$  with the taper length  $L_0$  of  $525 \mu\text{m}$ . A FMZI will be formed when a second taper of the same geometry is produced away from the first one with a spatial separation, which was  $54 \text{ mm}$  in this study. Part of the light energy in the fiber core will be coupled into the cladding through the first taper while the second taper will couple most of the cladding mode energy back into the core after passing through a section of fiber between the two tapers, in which part of the energy is attenuated during the cladding mode propagation. The phase difference  $\Phi$  between the core mode and the cladding mode can be approximated as  $\Phi=2\pi\Delta n_{\text{eff}}L/\lambda$ , where  $\Delta n_{\text{eff}}$  is the difference of the effective refractive indices between the core and the cladding modes,  $L$  is the distance between the two tapers, and  $\lambda$  is the operating wavelength. When the phase difference satisfies the condition  $\Phi=(2m+1)\pi$ , where  $m$  is the order of the Mach-Zehnder interference, the attenuation peak wavelength  $\lambda_m$  can be found at

$$\lambda_m = \frac{2\Delta n_{\text{eff}}L}{2m+1}. \quad (1)$$

The spacing between the adjacent attenuation peak wavelengths,  $\Delta\lambda_m$ , is

$$\Delta\lambda_m = \lambda_{m-1} - \lambda_m = \frac{4\Delta n_{\text{eff}}L}{(2m-1)(2m+1)}. \quad (2)$$

When the refractive index of the medium surrounding the fiber taper increases, the effective refractive index of the cladding mode increases by an amount denoted as  $\delta n_{\text{eff,RI}}$  and that of the core mode hardly disturbed. Therefore the difference of the effective refractive indices between the core and the cladding modes due to the ambient refractive index,  $\Delta n_{\text{eff,RI}}$ , decreases by  $\delta n_{\text{eff,RI}}$ . The attenuation peak wavelength  $\lambda_{m,\text{RI}}$  will change to a shorter wavelength  $\lambda_{m,\text{RI}}$  by  $\delta\lambda_{m,\text{RI}}$ , which is  $\delta\lambda_{m,\text{RI}}=2(\Delta n_{\text{eff,RI}}-\delta n_{\text{eff,RI}})L/(2m+1)-2\Delta n_{\text{eff,RI}}L/(2m+1)=-2\delta n_{\text{eff,RI}}L/(2m+1)$ .

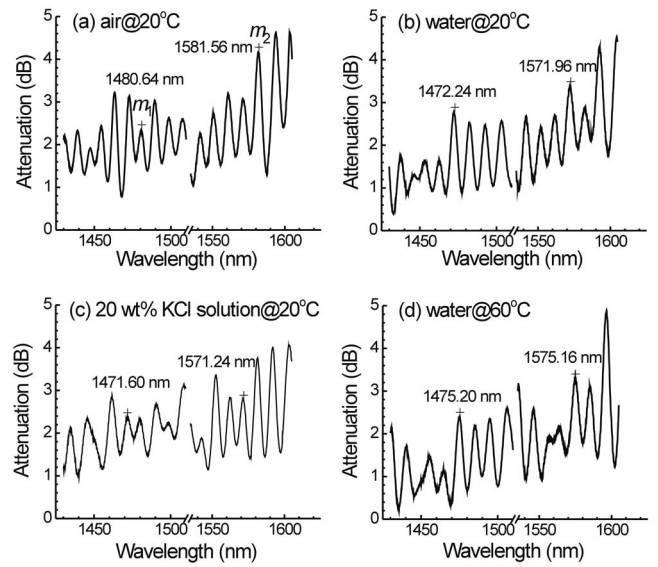


FIG. 2. Attenuation spectra of the FMZI at different environmental conditions: (a) in air at  $20^\circ\text{C}$ , (b) in water at  $20^\circ\text{C}$ , (c) in  $20 \text{ wt\%}$  KCl solution at  $20^\circ\text{C}$ , and (d) in water at  $60^\circ\text{C}$ .

In case the environmental temperature of the fiber tapers rises, both the effective refractive indices of the cladding mode and the core mode increase while that of the core mode changes more by  $\delta n_{\text{eff,T}}$  since the thermo-optic coefficient of the Ge-doped silica core is higher than that of the cladding consisting of fused silica. Consequently, the difference of the effective refractive index induced by the change in the environmental temperature ( $\Delta n_{\text{eff,T}}$ ) increases, as denoted by  $\delta n_{\text{eff,T}}$ . The attenuation peak wavelength  $\lambda_{m,T}$  shifts to a longer wavelength  $\lambda_{m,T'}$  by  $\delta\lambda_{m,T}$ , which is  $\delta\lambda_{m,T}=2(\Delta n_{\text{eff,T}}+\delta n_{\text{eff,T}})L/(2m+1)-2\Delta n_{\text{eff,T}}L/(2m+1)=2\delta n_{\text{eff,T}}L/(2m+1)$ .

In the experiment, the relationship between the attenuation peak wavelengths of the FMZI and the temperature was studied when the section containing the fiber taper pair was completely immersed in a water bath with a temperature resolution of  $0.1^\circ\text{C}$ . The response of the FMZI to the surrounding refractive index was investigated using KCl solution,<sup>21</sup> while the temperature of the solution was maintained at  $20.0 \pm 0.1^\circ\text{C}$ . At first the fiber tapers were placed in an environmental chamber at  $20^\circ\text{C}$  with the attenuation spectra of the two tandem fiber tapers from their transmission spectra shown in Fig. 2(a). Two interference orders were arbitrarily selected in the study, i.e., the interference order  $m_1$  (169) in the S-band with an attenuation peak wavelength  $\lambda_{m_1}$  of  $1480.64 \text{ nm}$  and a spacing  $\Delta\lambda_{m_1}$  of  $8.80 \text{ nm}$  and the interference order  $m_2$  (144) in the L-band with  $\lambda_{m_2}$  of  $1581.56 \text{ nm}$  and  $\Delta\lambda_{m_2}$  of  $11.04 \text{ nm}$ . The lower interference order  $m_2$  has a larger peak wavelength and spacing than those of the higher order  $m_1$ . When the fiber taper pair was transferred from ambient air to the water bath with the temperature maintained at  $20^\circ\text{C}$ , it was found from Fig. 2(b) that the peak wavelengths of the orders  $m_1$  and  $m_2$  blueshifted to  $1472.24$  and  $1571.96 \text{ nm}$ , respectively. Due to the decrease in  $\Delta n_{\text{eff,RI}}$  resulted from the increased surrounding refractive index from air (1.000) to water (1.333), the peak wavelengths of the orders  $m_1$  and  $m_2$  exhibit net shifts of  $8.40$  and  $9.60 \text{ nm}$ , respectively. Figure 2(c) shows the attenuation spectra of the fiber taper pair immersed in a  $20 \text{ wt\%}$  KCl solution at  $20^\circ\text{C}$  with a corresponding refractive index of

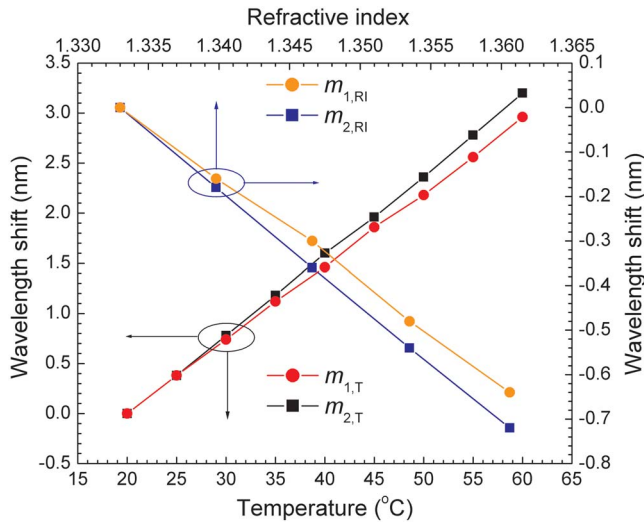


FIG. 3. (Color online) Dependences of the shifts of the attenuation peak wavelengths on refractive index and temperature for the interference orders  $m_1$  and  $m_2$ .

1.3606, which indicates that the two peak wavelengths of the orders  $m_1$  and  $m_2$  blueshifted to 1471.60 and 1571.24 nm, respectively. When the temperature of the water bath was varied from 20 to 60 °C, two peak wavelengths of the orders  $m_1$  and  $m_2$  both redshifted to 1475.20 and 1575.16 nm, respectively, as shown in Fig. 2(d). Redshifts of 2.96 and 3.20 nm in the peak wavelengths corresponding to the orders  $m_1$  and  $m_2$  have been identified, which take into consideration of the wavelength redshifts induced by the refractive index decrease of the water by 0.005 with the temperature increase of 40 °C.<sup>21</sup>

Figure 3 shows the dependences of the shifts in the peak wavelengths of the orders  $m_1$  and  $m_2$  on the changes in the refractive index and temperature. Compared with  $\lambda_{m1}$  in the S-band, the longer peak wavelength  $\lambda_{m2}$  in the L-band exhibits a larger shift under the same amount of change in the environmental parameter. Considering the shift due to the change in the refractive index of water with changing temperature, the sensitivities for  $m_1$  and  $m_2$  are  $-23.188$  and  $-26.087$  nm/RIU (refractive index unit) (blueshifts) for sensing refractive index, and  $0.071$  and  $0.077$  nm/°C (redshifts) for sensing temperature, respectively. It has been found that different interference orders have different FMZI peak wavelength gradients on temperature and refractive index. We define a character matrix  $M_{T,RI}$  to represent the sensing performance of the FMZI,

$$\begin{bmatrix} \Delta\lambda_1 \\ \Delta\lambda_2 \end{bmatrix} = M_{T,RI} \begin{bmatrix} \Delta T \\ \Delta n \end{bmatrix} = \begin{bmatrix} 0.071 & -23.188 \\ 0.077 & -26.087 \end{bmatrix} \begin{bmatrix} \Delta T \\ \Delta n \end{bmatrix}. \quad (3)$$

The character matrix  $M_{T,RI}$  can be used to simultaneously determine the variations in the temperature and the refractive index of the saline solution from the shifts of the attenuation peak wavelengths of the two arbitrarily selected interference orders  $m_1$  and  $m_2$ .

In conclusion, we have proposed and demonstrated an approach to realize simultaneous measurement of refractive index and temperature with a fiber Mach-Zehnder interferometry of high sensitivity. Compared with fiber grating and SPR sensors reported so far, the tapered fiber interferometer offers salient advantages of simple fabrication technique of low cost. The possibility to adjust the specifications of the taper configuration provides ample opportunity to satisfy requirements from different applications.

This work has been supported by the Natural Sciences and Engineering Research Council of Canada (NSERC DG312421-2008), Canada Research Chairs Program, Canada Foundation for Innovation, the Province of Newfoundland and Labrador, and the Memorial University of Newfoundland.

<sup>1</sup>M. Born and E. Wolf, *Principles of Optics*, 7th ed. (Cambridge University Press, Cambridge, 2005).

<sup>2</sup>*Surface Plasmon Resonance Based Sensors*, edited by J. Homola (Springer, Berlin, Heidelberg, 2006).

<sup>3</sup>M. G. Kuzyk, *Polymer Fiber Optics: Materials, Physics, and Applications* (CRC, Boca Raton, 2006).

<sup>4</sup>Ó. Esteban, M. Cruz-Navarrete, A. González-Cano, and E. Bernabeu, *Appl. Opt.* **38**, 5267 (1999).

<sup>5</sup>K. Mitsui, Y. Handa, and K. Kajikawa, *Appl. Phys. Lett.* **85**, 4231 (2004).

<sup>6</sup>Y.-J. He, Y.-L. Lo, and J.-F. Huang, *J. Opt. Soc. Am. B* **23**, 801 (2006).

<sup>7</sup>R. Falate, O. Frazão, G. Rego, J. L. Fabris, and J. L. Santos, *Appl. Opt.* **45**, 5066 (2006).

<sup>8</sup>Y.-P. Wang, D. N. Wang, W. Jin, Y.-J. Rao, and G.-D. Peng, *Appl. Phys. Lett.* **89**, 151105 (2006).

<sup>9</sup>Z. He, Y. Zhu, and H. Du, *Appl. Phys. Lett.* **92**, 044105 (2008).

<sup>10</sup>G. Nemova and R. Kashyap, *Opt. Lett.* **31**, 2118 (2006).

<sup>11</sup>Y. Y. Shevchenko and J. Albert, *Opt. Lett.* **32**, 211 (2007).

<sup>12</sup>N. Chen, B. Yun, and Y. Cui, *Appl. Phys. Lett.* **88**, 133902 (2006).

<sup>13</sup>A. P. Zhang, L.-Y. Shao, J.-F. Ding, and S. He, *IEEE Photonics Technol. Lett.* **17**, 2397 (2005).

<sup>14</sup>X. Chen, K. Zhou, L. Zhang, and I. Bennion, *Appl. Opt.* **44**, 178 (2005).

<sup>15</sup>A. Iadicco, S. Campopiano, A. Cutolo, M. Giordano, and A. Cusano, *Sens. Actuators B* **120**, 231 (2006).

<sup>16</sup>R. Jha, J. Villatoro, and G. Badenes, *Appl. Phys. Lett.* **93**, 191106 (2008).

<sup>17</sup>Z. Tian, S. S.-H. Yam, J. Barnes, W. Bock, P. Greig, J. M. Fraser, H.-P. Loock, and R. D. Oleschuk, *IEEE Photonics Technol. Lett.* **20**, 626 (2008).

<sup>18</sup>F. Xu and G. Brambilla, *Appl. Phys. Lett.* **92**, 101126 (2008).

<sup>19</sup>D. Monzón-Hernández, V. P. Minkovich, J. Villatoro, M. P. Kreuzer, and G. Badenes, *Appl. Phys. Lett.* **93**, 081106 (2008).

<sup>20</sup>J. M. Corres, F. J. Arregui, and I. R. Matias, *J. Lightwave Technol.* **24**, 4329 (2006).

<sup>21</sup>*Handbook of Chemistry and Physics*, 87th ed., edited by D. R. Lide (CRC, Boca Raton, 2007).